



Integrated Analysis of the ETS Family in Melanoma Reveals a Regulatory Role of ETV7 in the Immune Microenvironment

Hui Qu^{1†}, Hui Zhao^{2†}, Xi Zhang³, Yang Liu⁴, Feng Li¹, Liyan Sun¹ and Zewen Song^{3*}

¹ Department of Plastic Surgery, Shanxi Bethune Hospital, Shanxi Academy of Medical Sciences, Taiyuan, China,

² Department of Urology, The Affiliated Hospital of Weifang Medical University, Weifang, China, ³ Department of Oncology, The Third Xiangya Hospital of Central South University, Changsha, China, ⁴ Department of Pathology, The Third Xiangya Hospital of Central South University, Changsha, China

OPEN ACCESS

Edited by:

Lidia Karabon,
Hirsfeld Institute of Immunology and
Experimental Therapy (PAS), Poland

Reviewed by:

Peter Hollenhorst,
Indiana University, United States
Jia Li,
Shanghai University of Traditional
Chinese Medicine, China

*Correspondence:

Zewen Song
xy3szw@163.com

[†]These authors have contributed
equally to this work

Specialty section:

This article was submitted to
Cancer Immunity
and Immunotherapy,
a section of the journal
Frontiers in Immunology

Received: 30 September 2020

Accepted: 19 November 2020

Published: 23 December 2020

Citation:

Qu H, Zhao H, Zhang X, Liu Y, Li F,
Sun L and Song Z (2020) Integrated
Analysis of the ETS Family in Melanoma
Reveals a Regulatory Role of ETV7
in the Immune Microenvironment.
Front. Immunol. 11:612784.
doi: 10.3389/fimmu.2020.612784

The ETS family modulates immune response and drug efficiency to targeted therapies, but their role in melanoma is largely unclear. In this study, the ETS family was systematically analyzed in multiple public data sets. Bioinformatics tools were used to characterize the function of ETV7 in melanoma. A prognostic model was constructed using the LASSO Cox regression method. We found that ETV7 was the only differentially expressed gene with significant prognostic relevance in melanoma. Enrichment analysis of seven independent data sets indicated ETV7 participation in various immune-related pathways. ETV7 particularly showed a strong positive correlation with CD8+ T cell infiltration. The prognostic model based on ETV7 and its hub genes showed a relatively good predictive value in training and testing data sets. Thus, ETV7 can potentially regulate the immune microenvironment in melanoma.

Keywords: ETS family, melanoma, ETV7, immune microenvironment, CD8+ T cell, single-cell RNA sequencing

INTRODUCTION

Melanoma, originating from pigment-producing melanocytes, comprises 75% of deaths related to skin cancer (1). In 2019, a total of 96,480 new cases of melanoma of the skin reported were in the United States (2). At its early stage, the disease could be surgically removed, with a relatively good prognosis; however, when it spreads to distant organs, the 5-year survival rate of patients with this disease sharply declines to roughly 10%, as indicated by a recent review (3). Targeted therapies and immune checkpoint inhibitors (ICIs) have revolutionized the treatment of metastatic melanoma. However, numerous problems still need to be addressed. For instance, current evidence suggests that 40 to 65% of patients with advanced-stage metastatic melanoma show minimal or no RECIST response to ICIs at the outset (*de novo* resistance), and 43% of responders acquire resistance by 3 y (4, 5). Moreover, melanoma patients receiving mitogen-activated protein kinase (MAPK)-targeted therapy also develop resistance, which leads to relapse (6). Several underlying mechanisms have been revealed, such as NRAS mutations and BRAF amplification, but 40% of them present unknown resistance mechanisms beyond genetic alterations (6–8).

Recent studies find that transcriptional factors (TFs) relevant to the MAPK pathways modulate drug efficiency to MAPK inhibitors (9, 10). For instance, overexpression of ETV1, ETV4, or ETV5 can sufficiently restore cell proliferation in the presence of trametinib, a MEK inhibitor (9). An early study also observes that overexpression of ETV1 confers resistance to MAPK inhibitors in BRAF-mutant melanoma (11). ETV1, ETV4, and ETV5 are members of the E26 transformation-specific or E-twenty-six (ETS) family, which is one of the largest transcriptional factor families and participates in multiple biological processes such as cellular differentiation, cell cycle control (12), cell migration (13), and cell proliferation (14). The family consists of 28 TFs in humans and binds to similar DNA sequences of MAPK (15). Various studies have revealed that aberrant expression of many ETS family members is strongly associated with tumor initiation, progression, and metastasis in cancer (16–18). Some ETS inhibitors, such as VPC-18005 and BRD32048, exert antitumor effects in pre-clinical studies (19, 20). In skin melanoma, the function of the ETS family is poorly studied. ETS1 can promote aggregation and invasion of melanoma (21, 22), and ETV2 is required during tumor angiogenesis (23); meanwhile, the role of the rest of the ETS family members is largely unclear.

In addition, the ETS family has been shown to play a role in immunity (24–26). ELF1, ETV4, ETV3L, ETS1, and ETS2 can up-regulate the expression of leukocyte-associated immunoglobulin-like receptor-1, which inhibits the maturation, differentiation, and activation of immune cells (25, 27). ELF4 can inhibit the proliferation of naive CD8+ T cells by increasing the expression of KLF4 (24, 28). However, the regulation of immune response in cancer by ETS family members, as well as the mechanism underlying this regulation, has yet to be determined.

In the current study, we systematically assessed the expression profile, prognostic significance, and role of ETS family members in human skin cutaneous melanoma (SKCM) by integrating data from The Cancer Genome Atlas (TCGA) database, the Genotype–Tissue Expression (GTEx) Project, Oncomine database, cBioPortal database, and Gene Expression Omnibus (GEO) database. Our results indicate that ETV7 is markedly downregulated in melanoma, and low ETV7 expression is related to the poor prognosis of SKCM patients. Enrichment analysis and immune profile analysis indicate that ETV7 may regulate the differentiation and activation of T cells. This finding suggests a previously unrecognized involvement of ETV7 in immunity and the potential of the gene to modulate the immune response to the disease.

MATERIALS AND METHODS

Data Acquisition and Processing

The workflow of this study is presented in **Figure 1**. The TCGA_SKCM data set and GEO data sets (GSE65904 and GSE19234) were acquired and processed using the method described in our previous study (29). After data filtering was conducted, 448 tumor samples with survival data in the TCGA_SKCM data set, 210 tumor samples in GSE65904, and 44 samples in GSE19234 were used for further analysis. The single-cell RNA sequencing data (GSE72056) were downloaded and analyzed directly in the current study because the data had been processed and normalized (30). All data used in the present study were acquired from public databases, requiring no further approval by an ethics committee.

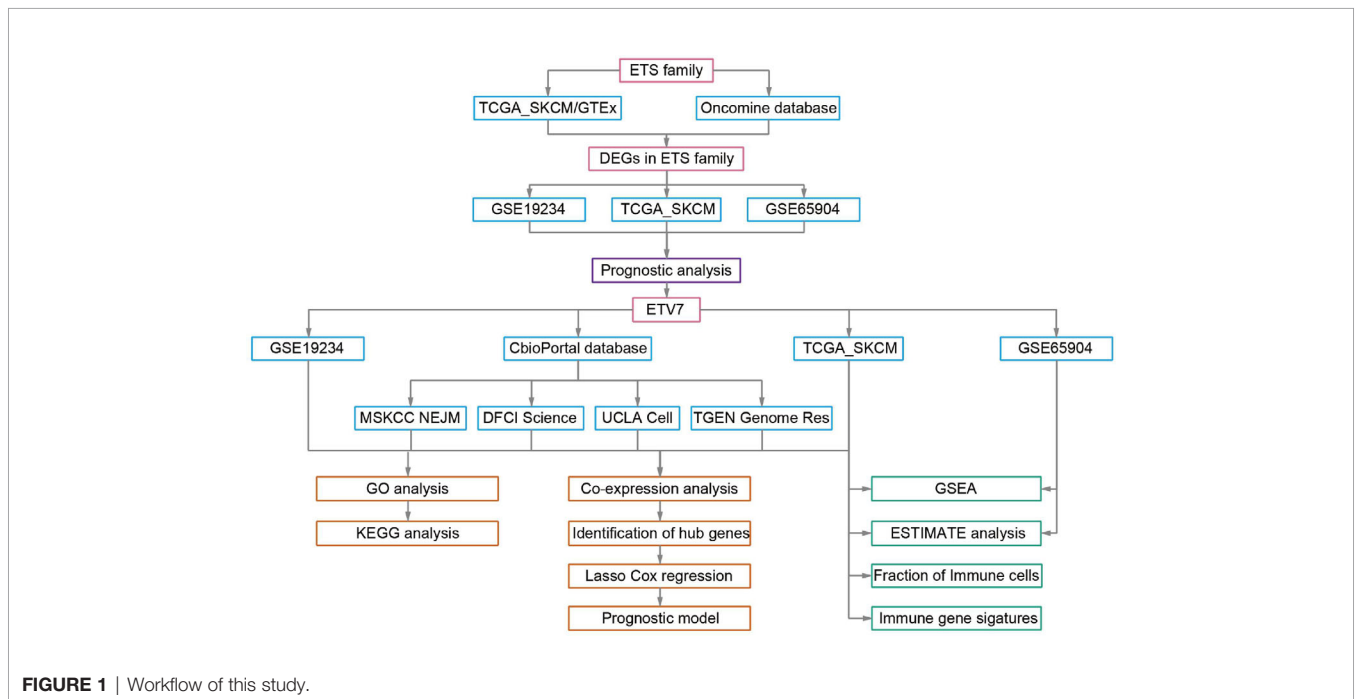


FIGURE 1 | Workflow of this study.

Online Database Analysis

The Oncomine database (<https://www.oncomine.org/resource/login.html>) was used to validate the transcription level of the genes of interest in skin melanoma by retrieving expression data (log₂-transformed) in three cohorts of melanoma vs. normal tissues for statistical comparison, with the following default thresholds: P-value < 1E-4, fold change >2, and gene ranks in the top 10%.

The GEPIA2 (<http://gepia2.cancer-pku.cn/>) database was also used to compare the transcript level of the genes of interest between melanoma tumors and normal samples from TCGA and GTEx projects.

The cBioPortal for Cancer Genomics (<http://www.cbioportal.org/>) was used to identify genes that exhibit a strong positive correlation ($R > 0.5$, q-value < 0.05) with ETV7 in all available melanoma-related data sets with gene expression data.

The human protein atlas (<https://www.proteinatlas.org/>) was used to analyze the expression of ETV7 across a set of normal human cells or tissues.

Functional Analysis and Enrichment Analysis

The co-expressed genes of ETV7 shared in five independent data sets were constructed into a protein–protein interaction (PPI) network in the STRING database (<http://string-db.org>). Cytoscape version 3.7.2 was used to visualize these networks. Hub genes were identified as the top 10 nodes, based on the score generated by the cytoHubba plugin in Cytoscape (ranked by degree).

Gene ontology (GO) and Kyoto Encyclopedia of Genes and Genomes (KEGG) enrichment analyses were conducted using the clusterProfiler package in R version 3.6.2 (18).

Gene set enrichment analysis (GSEA) was used to investigate pathways enriched in the high- and low-ETV7 groups. *C2.cp.kegg.v7.1.symbols.gmt* was chosen as the gene set database. The pathways were considered significantly enriched with the following criteria: nominal p-value < 0.05, false discovery rate q-value < 0.25, and normalized enrichment score > 1.

Immune Profile Analysis

The immune and stromal scores of each sample were estimated using the ESTIMATE algorithm in the ‘estimate’ package in R version 3.6.2 (31). Immune cell infiltration in each sample of the TCGA_SKCM data set was conducted by preparing and uploading gene expression data into the TIMER2.0 website (<http://timer.cistrome.org/>) in accordance with the instruction on the website (32).

Construction of the Prognostic Model

The least absolute shrinkage and selection operator (LASSO) Cox regression analysis was conducted using the glmnet package in R. The analysis generated key gene signatures and their corresponding coefficients, which were used to calculate the novel score, as follows: score = $-0.08241781 \times \text{CCR5} - 0.01208383 \times \text{IFNG} - 0.13002695 \times \text{TBX21} - 0.04765633 \times \text{CXCL10} - 0.33444001 \times \text{CXCR3} - 0.05630411 \times \text{CCL5}$. To facilitate the interpretation of results from different data sets, the risk score

was calculated by subtracting the minimum score of the cohort from this score, and dividing the difference by the absolute value of the maximum score of the cohort—that is, namely, risk score = $(\text{score} - \text{Min})/\text{absolute}(\text{Max})$.

Statistical Analysis

The data collected were analyzed by default as described using web resources. The remaining data were analyzed using R version 3.6.2. The median expression of genes or the median value of the risk score was used as cutoff value in dividing patients into two subgroups. Univariate Cox regression and multivariate Cox regression were conducted using the survminer package in R. The survival analyses were compared using the Kaplan–Meier method with the logrank test. Time-dependent receiver operator characteristic (ROC) analyses and subsequent calculation of the area under the curve (AUC) were performed using the timeROC package in R. Correlation analysis between the gene expression of ETV7 and that of the remaining genes was conducted by R software version 3.6.2 with spearman method. Wilcoxon test was conducted to compare gene expression between groups. Packages in R used for data analysis and graph plotting included ggplot2, ggpubr, limma, vennDiagram, tidyverse, rms, org.Hs.eg.db, dplyr, Rtsne, and plyr. P < 0.05 was considered statistically significant (*, P < 0.05; **, P < 0.01; ***, P < 0.001; ****, P < 0.0001).

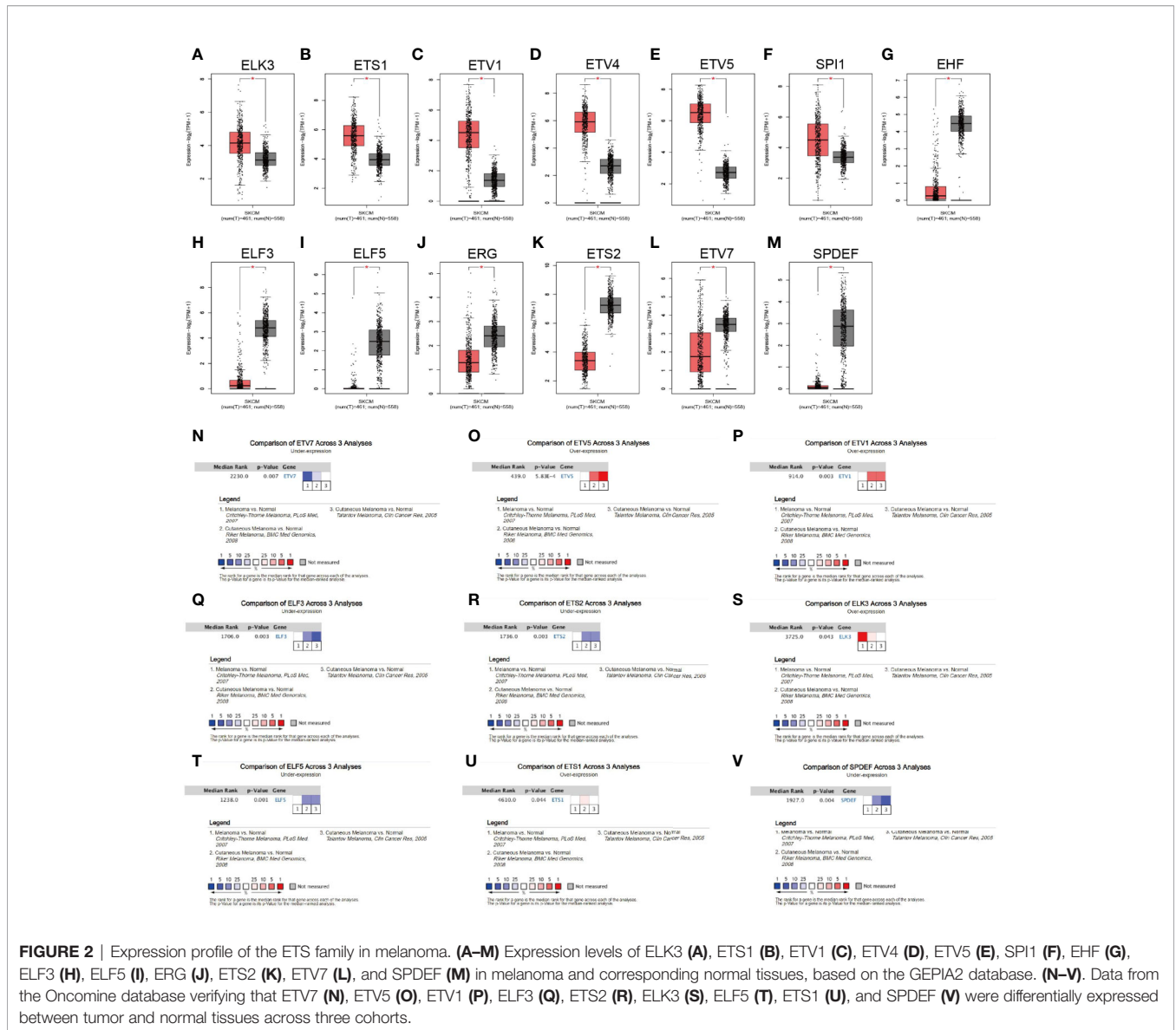
RESULTS

Identification of Differentially Expressed ETS Family Members in Melanoma

The TCGA_SKCM project has only one normal sample. Thus, we first investigated the expression of all ETS family members in melanoma and normal skin by manipulating the data from the GTEx database. GEPIA2 integrates gene expression data from the TCGA and GTEx projects *via* a standard processing pipeline (33). Using the default cutoff value of GEPIA2 ($|\text{Log2FC}|$ cutoff = 1, and q-value cutoff = 0.01), we found that 13 of the 28 family members were differentially expressed (**Figures 2A–M**, **Supplementary Figures 1A–O**). In particular, ELK3, ETS1, ETV1, ETV4, ETV5, and SPI1 were significantly upregulated in melanoma (**Figures 2A–F**), whereas EHF, ELF3, ELF5, ERG, ETS2, ETV7, and SPDEF were significantly downregulated in the tumor (**Figures 2G–M**). Further, the expression profiles of ETV1, ETV5, ETV7, ELF3, ETS1, ETS2, ELK3, ELF5, and SPDEF were validated by comparing their transcriptional level between melanoma and normal tissues across three independent cohorts from the Oncomine database (**Figures 2N–V**). However, the remaining members were not differentially expressed between tumor and normal tissues (**Supplementary Figures 1P–S**).

ETV7 as an Independent Prognostic Predictor in Melanoma

We subsequently evaluated the prognostic significance of the above nine differentially expressed ETS family members in TCGA_SKCM. Analysis suggested that ETV7 exhibited



prognostic significance in melanoma patients (Figures 3A–H). Moreover, melanoma patients with high ETV7 showed significantly longer disease-specific survival (DSS) than those with low ETV7 ($p < 0.0001$, Figure 3I). We further evaluated the prognostic relevance of these nine differentially expressed genes (DEGs) in the GSE65904 data set and found a similar result for ETV7 ($p = 0.038$, Figure 3J). By contrast, the remaining genes showed no prognostic significance (Supplementary Figures 2A–H). In addition, data from the GSE19234 data set showed that melanoma patients with low ETV7 had significantly shorter survival time since metastasis ($p = 0.045$, Figure 3K).

As shown in Table 1, univariate Cox regression analysis indicated that low ETV7 ($p < 0.001$), age > 60 y ($p < 0.001$), Breslow depth > 2 cm ($p < 0.001$), Clark level IV–V ($p < 0.001$), non-White patients ($p = 0.004$), advanced stage (III–IV, $p < 0.001$), advanced T stage (T3–Tx, $p < 0.001$), and advanced N stage (N1–Nx, $p < 0.001$) are associated with shorter OS. In

addition to the M stage, these factors underwent multivariate Cox regression analysis. The result showed that ETV7 and the N stage remained to be independent risk factors (Table 1).

We then investigated the prognostic relevance of ETV7 in different subgroups of melanoma patients. As shown in Figures 4A, B, low ETV7 expression was correlated with a significantly short OS in melanoma patients younger than 60 y (Figure 4A, $p = 0.0017$) or older than 60 y (Figure 4B, $p = 0.031$). A similar association between ETV7 and survival time was also observed in both male and female patients (Figures 4C, D), patients with different T, N, and M stages (Figures 4E, F), and patients with melanoma at the early (Figure 4K, $p = 0.0047$) or advanced (Figure 4L, $p = 0.015$) stage.

Coexpression and Enrichment Analysis

The aforementioned analysis indicated that ETV7 was significantly downregulated in melanoma and was associated

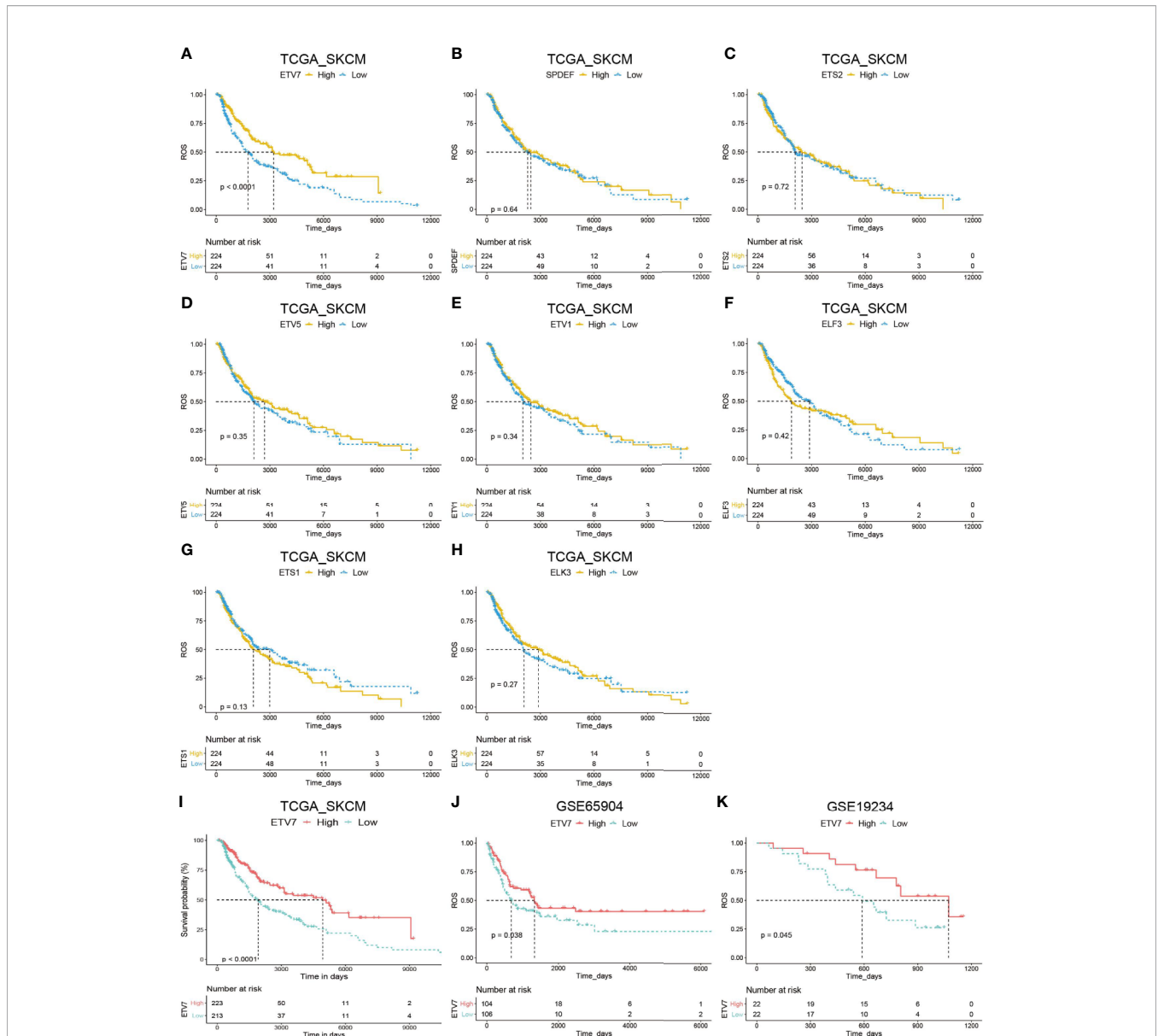


FIGURE 3 | Prognostic analysis of DEGs of the ETS family in melanoma. **(A–H)** Kaplan–Meier plot of overall survival (OS) in melanoma patients in the TCGA_SKCM cohort with high and low expression of ETV7 **(A)**, SPDEF **(B)**, ETS2 **(C)**, ETV5 **(D)**, ETV1 **(E)**, ELF3 **(F)**, ETS1 **(G)**, and ELK3 **(H)**. **(I)** Kaplan–Meier plot of DDS of melanoma patients in the TCGA_SKCM cohort with high and low expression of ETV7. **(J)** Kaplan–Meier plot of DDS of melanoma patients in the GSE65904 cohort with high and low expression of ETV7. **(K)** Kaplan–Meier plot of survival time since metastasis of melanoma patients in the GSE19234 cohort with high and low expression of ETV7.

with the prognosis of melanoma patients. To understand the function of ETV7 in melanoma, we first identified the ETV7-related genes, which were defined as those exhibiting strong correlation (coefficient ≥ 0.5 , $p < 0.05$) with ETV7 at the transcriptional level in melanoma. A total of 623 ETV7-related genes were found in the TCGA_SKCM data set (**Supplementary Table 1**). GO analysis indicated that these genes were enriched in immune-related biological processes and molecular functions such as T cell activation, regulation of T cell activation, regulation of lymphocyte activation, response to interferon-gamma, regulation of

leukocyte proliferation, MHC protein binding, cytokine receptor activity, chemokine receptor binding, MHC class II receptor activity, and CCR chemokine receptor binding (**Supplementary Figure 3A**). KEGG analysis suggested that these genes were enriched in antigen processing and presentation, cell adhesion molecules, cytokine–cytokine receptor interaction, Th1 and Th2 cell differentiation, Th17 cell differentiation, chemokine signaling pathway, natural killer (NK) cell-mediated cytotoxicity, and PD-L1 expression and PD-1 checkpoint pathway in cancer (**Figure 5A, Supplementary Table 2**).

TABLE 1 | Univariate and multivariate Cox regression analyses of ETV7 and clinicopathologic features in melanoma patients.

Clinicopathologic variable	Univariate cox analysis		Multivariate cox analysis	
	HR (95% CI)	p-value	HR (95% CI)	p-value
ETV7 (low vs. high)	1.709 (1.303–2.242)	<0.001	1.529 (1.072–2.182)	0.019
Age (<60 vs. ≥60)	0.619 (0.469–0.915)	<0.001	0.721 (0.507–1.024)	0.068
Breslow depth (<2 mm vs. ≥2 mm)	0.449 (0.327–0.615)	<0.001	0.498(0.223–1.113)	0.089
Clark level (I–III vs. IV–V)	0.488 (0.344–0.693)	<0.001	0.755 (0.499–1.144)	0.186
Race (White vs. non-White)	0.349 (0.171–0.711)	0.004	0.684 (0.093–5.027)	0.709
Stage (0–II vs. III–IV)	0.589 (0.441–0.785)	<0.001	1.290 (0.678–2.452)	0.438
T (T0–T2 vs. T3–TX)	0.583 (0.435–0.782)	<0.001	1.282 (0.559–2.939)	0.558
N (N0 vs. N1–NX)	0.604 (0.458–0.796)	<0.001	0.370 (0.198–0.691)	0.002
M (M0 vs. M1/MX)	0.582 (0.307–1.103)	0.097	0.533 (0.189–1.506)	0.235
Gender (male vs. female)	1.134 (0.855–1.503)	0.383	–	–
Multiple primary tumors present (No vs. YES)	0.647 (0.342–1.224)	0.181	–	–
Prior systemic therapy (No vs. YES)	1.356 (0.826–2.228)	0.229	–	–
Radiation therapy (No vs. YES)	1.753 (0.836–3.678)	0.138	–	–
Prior malignancy diagnoses (No vs. YES)	0.851 (0.485–1.493)	0.573	–	–

We further searched the cBioportal database and found that in addition to the TCGA_SKCM data set, four of nine melanoma-related data sets contained gene expression data: *MSKCC NEJM*, *DFCI Science*, *UCLA Cell*, and *TGEN Genome Res*. Coexpression analysis of ETV7 in these four data sets identified 1 021 ETV7-related genes in the *MSKCC NEJM* cohort, 981 genes in the *DFCI Science* cohort, 440 genes in the *UCLA Cell* cohort, and 667 genes in the *TGEN Genome Res* cohort. The GO and KEGG analyses of these genes in each cohort consistently indicated that they were enriched in similar immune-related processes or pathways (**Figures 5B–E, Supplementary Figures 3B–E**). The coexpression and subsequent GO and KEGG analyses of GSE19234 further verified the association between ETV7 and immune-related pathways (**Figure 5F, Supplementary Figure 3F**).

In addition, GSEA was applied to investigate the difference in signaling pathways between the low and high ETV7 expression subgroups in the TCGA_SKCM and GSE65904 data sets. The results inferred that various immune-related pathways were enriched in the high ETV7 expression subgroups. These pathways included antigen processing and presentation, Toll-like receptor signaling pathway, T cell receptor signaling pathway, RIG-I like receptor signaling pathway, JAK-STAT signaling pathway, B cell receptor signaling pathway, NK cell-mediated cytotoxicity, cytokine-cytokine receptor interaction, and Fc gamma R-mediated phagocytosis (**Figures 6A–I, Supplementary Table 3**).

Immune Profile

The aforementioned analysis suggests a close link between ETV7 and immune-related pathways. We thus employed the ESTIMATE method to evaluate the overall TME status in the high- and low-ETV7 subgroups of melanoma patients. In the TCGA_SKCM and GSE65904 cohorts, the immune and stromal scores were significantly higher in the high-ETV7 subgroups than in the low-ETV7 subgroups (**Figures 7A, B**). All phenotypic

and functional markers of T cells—CD3E, CD4, CD8B, FOXP3, GZMB, PRF1 and TBX21—were expressed at higher levels in melanoma patients with high ETV7 expression (**Figure 7C**). Notably, the inhibitory immune receptors or ligands (CTLA4, LAG3, and PDCD1) and activating immune receptors (CD27, CD40, CD80, ICOS, TNFRSF4, and TNFRSF9) were significantly elevated in patients with high ETV7 expression, indicating a complex immune response in this subgroup (**Figures 7D, E**). Among the immune modulators, ENTPD1 was highly expressed in the high-ETV7 subgroup of melanoma patients, whereas NT5E showed no significant difference (**Figure 8F**). Moreover, IFN γ signatures (CXCL10, CXCL9, IDO1, IFNG, and STAT1) and myeloid lineage phenotypic and functional markers (CD14, CD163, CD33, and CD68) were also significantly increased in melanoma patients with high ETV7 (**Figures 7G, H**). However, ARG1, a previously reported M2 macrophage marker, was not differently expressed in the two subgroups (**Figure 7H**).

Further, multiple immune deconvolution methods—namely, TIMER, QUANTISEQ, CIBERSORT, MCPOUNTER, XCELL, and EPIC—were manipulated to estimate the abundances of immune cells infiltrating into melanoma (34, 35). Analyzing the relationship between ETV7 and the abundance of different immune cells, we observed a strong positive correlation between ETV7 and CD8+ T cells, as determined by TIM (**Figure 8A**, $r = 0.56$, $p < 2.2 \times 10^{-16}$), QUANTISEQ (**Figure 8B**, $r = 0.6$, $p < 2.2 \times 10^{-16}$), CIBERSORT (**Figure 8C**, $r = 0.6$, $p < 2.2 \times 10^{-16}$), CIBERSORT-ABS (**Figure 8D**, $r = 0.66$, $p < 2.2 \times 10^{-16}$), MCPOUNTER (**Figure 8E**, $r = 0.58$, $p < 2.2 \times 10^{-16}$), EPIC (**Figure 8F**, $r = 0.41$, $p < 2.2 \times 10^{-16}$), and XCELL (**Figure 8G**, $r = 0.63$, $p < 2.2 \times 10^{-16}$). In addition, ETV7 exhibited a strong positive correlation with CD8+ effector-memory T cells (**Figure 8H**, $r = 0.6$, $p < 2.2 \times 10^{-16}$) and CD8+ central memory T cells (**Figure 8I**, $r = 0.66$, $p < 2.2 \times 10^{-16}$).

Previous studies indicate that ETV7 is predominantly expressed in hematopoietic tissues (36, 37); thus, the strong positive correlation between ETV7 and CD8+ T cell infiltration

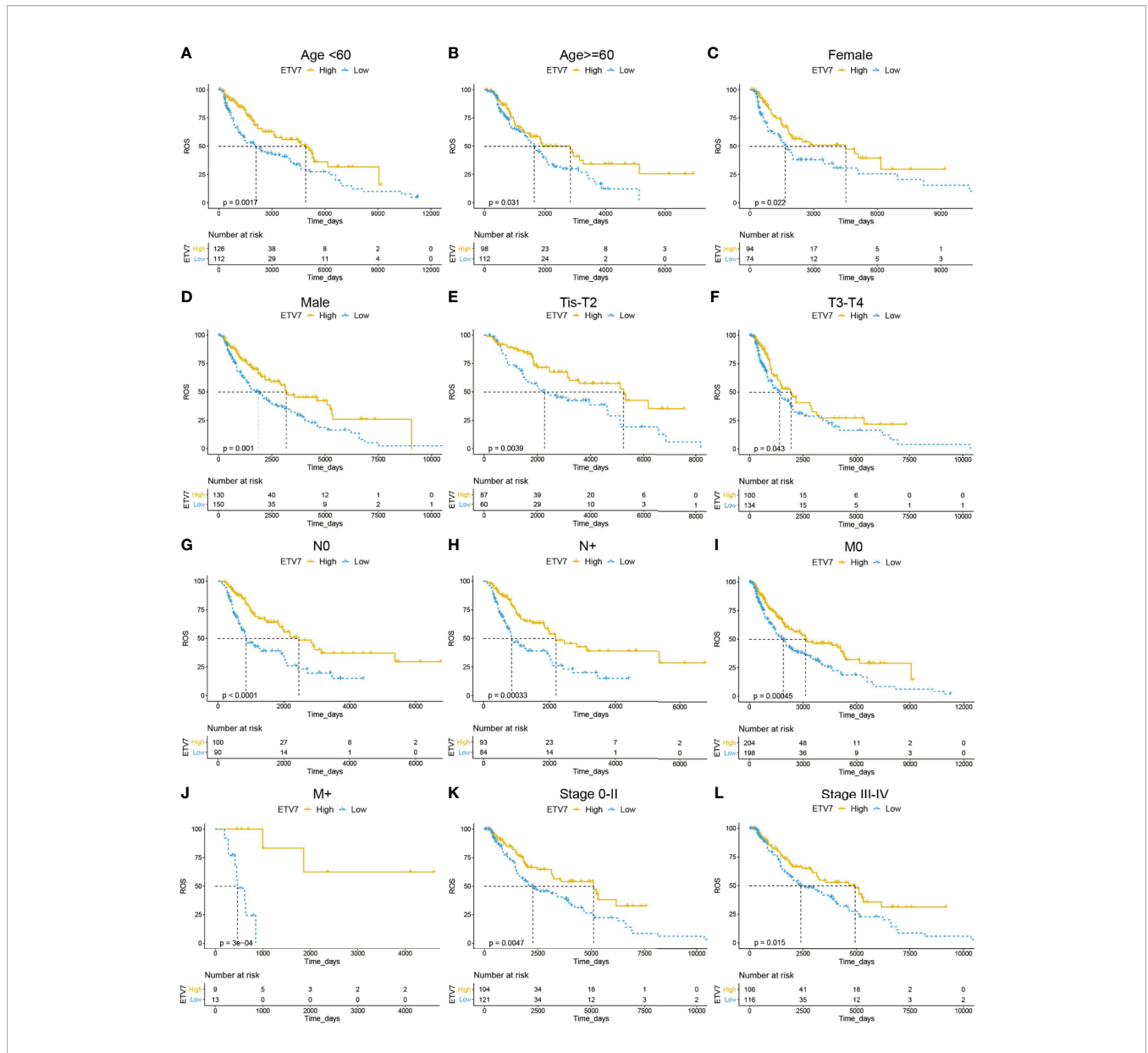


FIGURE 4 | Prognostic analysis of ETV7 in different subgroups of melanoma patients. **(A, B)** Kaplan–Meier plot of OS in high and low-ETV7 subgroups of melanoma patients < 60 y **(A)** or older than 60 y **(B)**. **(C, D)** Kaplan–Meier plot of overall survival (OS) in female **(C)** or male **(D)** melanoma patients with high and low expression of ETV7. **(E, F)** Kaplan–Meier plot of OS in high and low-ETV7 subgroups of melanoma patients at early (Tis–T2, **E**) or advanced (T3–T4, **F**) T stage. **(G, H)** Kaplan–Meier plot of OS in high and low-ETV7 subgroups of melanoma patients with **(G)** or without **(H)** lymph node metastasis. **(I, J)** Kaplan–Meier plot of OS in high- and low-ETV7 subgroups of melanoma patients with **(I)** or without **(J)** distant metastasis. **(K, L)** Kaplan–Meier plot of OS in high- and low-ETV7 subgroups of melanoma patients at the early **(K)** or advanced **(L)** stage.

may be attributed to ETV7 expression in this subgroup of T cells. To test this hypothesis, we analyzed the GSE72056 data set, a public single-cell RNA sequencing (scRNA-seq) data set of melanoma patients (30). In this data set, the tumor cells were designated by copy number variation analysis, whereas the non-malignant cells were annotated as six types of cells—T cells, B cells, macrophages, endothelial cells, cancer-associated fibroblasts, and NK cells—based on preferentially or uniquely expressed marker genes (30). The remaining unresolved cells

were referred to as undefined cells in the current study. Consistent with the original study by Itay Tirosh et al. (30), non-linear dimensionality reduction (t-distributed stochastic neighbor embedding (t-SNE)) analysis revealed that these eight clusters of cells could be distinguished separately (**Figure 9A**). Tumor cells exhibited markedly elevated expression of MLANA, a widely used biomarker of melanoma (**Figure 9B**). CD2 was exclusively expressed in T cells (**Figure 9C**), macrophages had distinct CD163 expression (**Supplementary Figure 4A**), and B

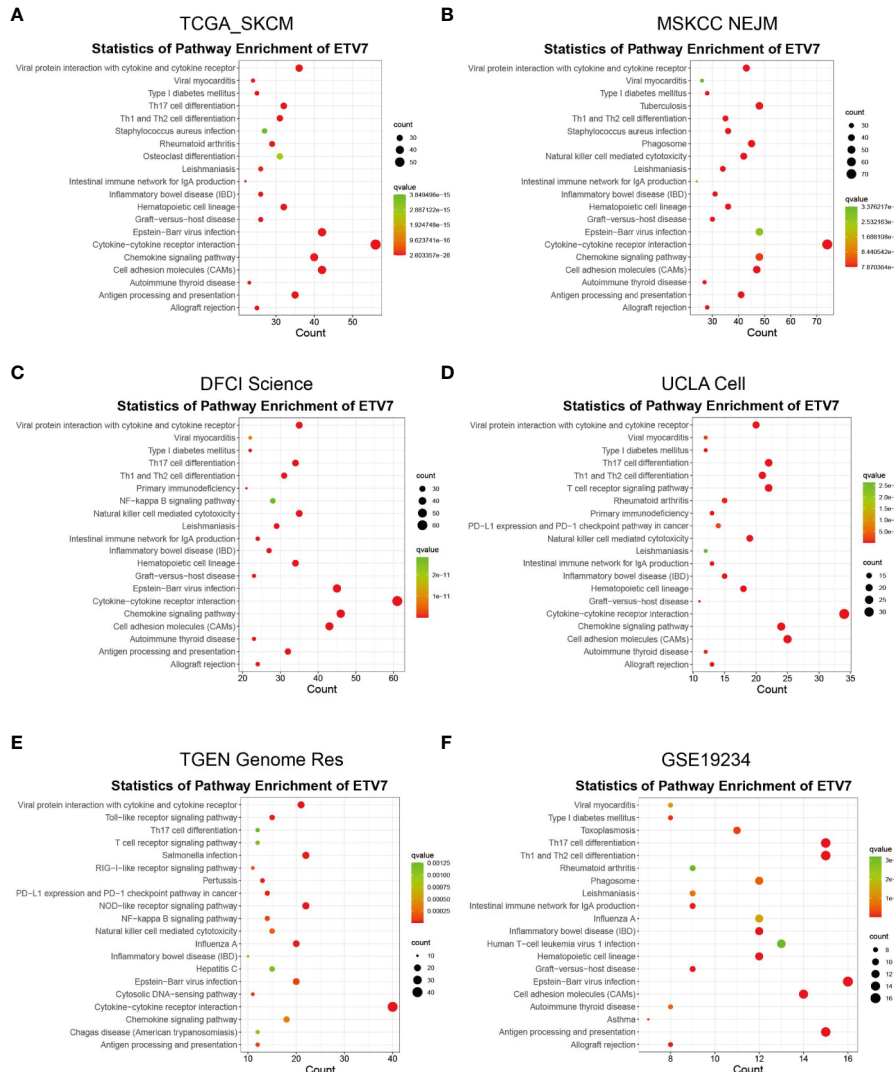


FIGURE 5 | KEGG analysis of ETV7-related genes in TCGA_SKCM (A), MSKCC_NEJM (B), DFCI Science (C), UCLA Cell (D), TGEN Genome Res (E), and GSE19234 (F) data sets.

cells were marked by CD19 expression (Supplementary Figure 4B) (30). As shown in Figure 9D, ETV7 was not exclusively expressed in T cells but could be detected in several types of cells, including tumor cells (green circle), T cells, and macrophages. ETV7 was also not detected in most CT8+ T cells (labeled as CD8A+ and/or CD8B+, Figures 9D–F), and a negligible fraction of ETV7-positive T cells (Figures 9D–F, blue circle) were not recognized as CD8+ T cells. Collectively, these results indicate that the strong positive correlation between ETV7 and infiltration of CD8+ T cells cannot be attributed to ETV7 expression in these cells. In addition, we found that skin (green block, Figure 9G) showed the highest ETV7 expression across a set of normal human cells or tissues, including T cells (denoted by a blue block, Figure 9G, Supplementary Figure 4C).

Construction of an ETV7-Related Prognostic Model

As shown in Figure 10A, 98 genes are commonly shared among the ETV7-related genes in the five aforementioned data sets. A PPI network was constructed in the STRING database and visualized in Cytoscape (Figure 10B). Consistent with the results of GO, KEGG, and GSEA analyses, ClueGo analysis demonstrated that these 98 genes were predominantly involved in immune-related biological processes such as T cell activation, chemokine-mediated signaling pathway, T cell differentiation, and response to interferon-gamma (Figures 10C, D), as well as in immune-related pathways such as the T cell receptor signaling pathway, cytokine-cytokine receptor interaction, and TNF signaling pathway (Figures 10E, F) (38). The 10 hub genes

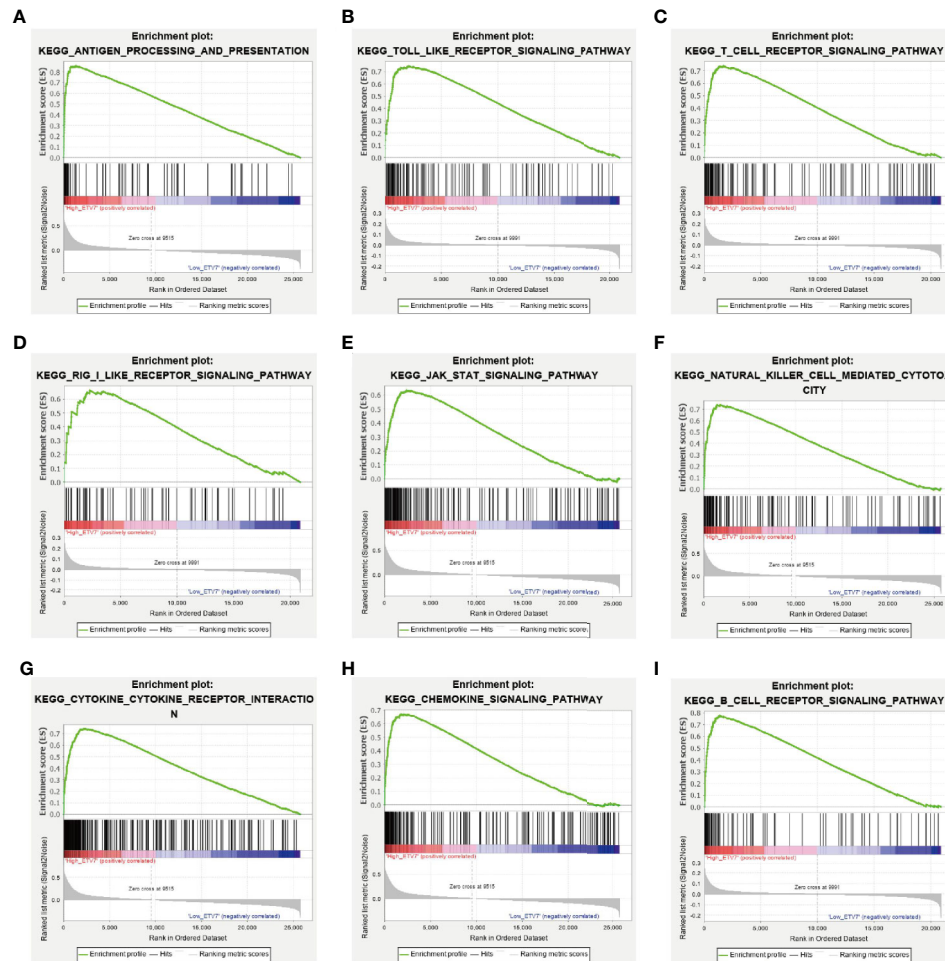


FIGURE 6 | GSEA between melanoma patients with high and low ETV7 expression in the TCGA_SKCM and GSE65904 cohorts (A–I).

were identified as CCR5, IFNG, TBX21, CXCL10, PRF1, CD2, CXCR3, CXCL9, CCL5, IL15 (Figure 10B). All melanoma patients exhibiting low expression of these hub genes showed a significantly shorter OS (Supplementary Figures 5A–J).

To construct an ETV7-related prognostic model for the disease-specific survival of melanoma patients, ETV7 and 10 hub genes were input into a LASSO Cox regression model in the GSE65904 data set (n = 210). Six genes were selected using the partial likelihood deviance method (Figures 11A, B). These genes were CCR5, IFNG, TBX21, CXCL10, CXCR3, and CCL5. The risk score was calculated by inputting the selected signature genes into the aforementioned formula. The median value of the risk score was set as the cutoff value, dividing patients into low- and high-risk subgroups. Prognostic analysis with the Kaplan–Meier method showed that melanoma patients with low risk scores had a significantly longer DSS (Figure 11C, p = 0.0047) in the GSE65904 cohort. Time-dependent ROC analysis in this cohort demonstrated that the risk score had a favorable predictive value (Figure 11D, AUC at 1 year = 0.64, AUC at 3 y = 0.69). The prognostic value of the established risk score was

validated in the TCGA cohort (Figure 11E, p < 0.0001). The ROC analysis in this data set showed that the AUC at 1 y reached 0.7 and at 3 y was 0.65 (Figure 11F). Further, melanoma patients with high risk scores showed significantly shorter survival times since metastasis than those with low risk scores in the GSE19234 cohort (p = 0.021, Figure 11G). The ROC analysis in this data set indicated that the AUC at 1 y reached 0.69 and at 3 y was 0.98 (Figure 11H).

DISCUSSION

In this systematic analysis of the ETS family in melanoma, we first integrated the data from the TCGA and GTEx databases and three available cohorts of melanoma patients in the OncoPrint database; we then found that ELK3, ETS1, ETV1, and ETV5 were significantly upregulated in melanoma, whereas ELF3, ELF5, ETS2, ETV7, and SPDEF were significantly downregulated in the tumor. Prognostic analysis of these DEGs in the TCGA_SKCM and GSE65904 data sets consistently showed

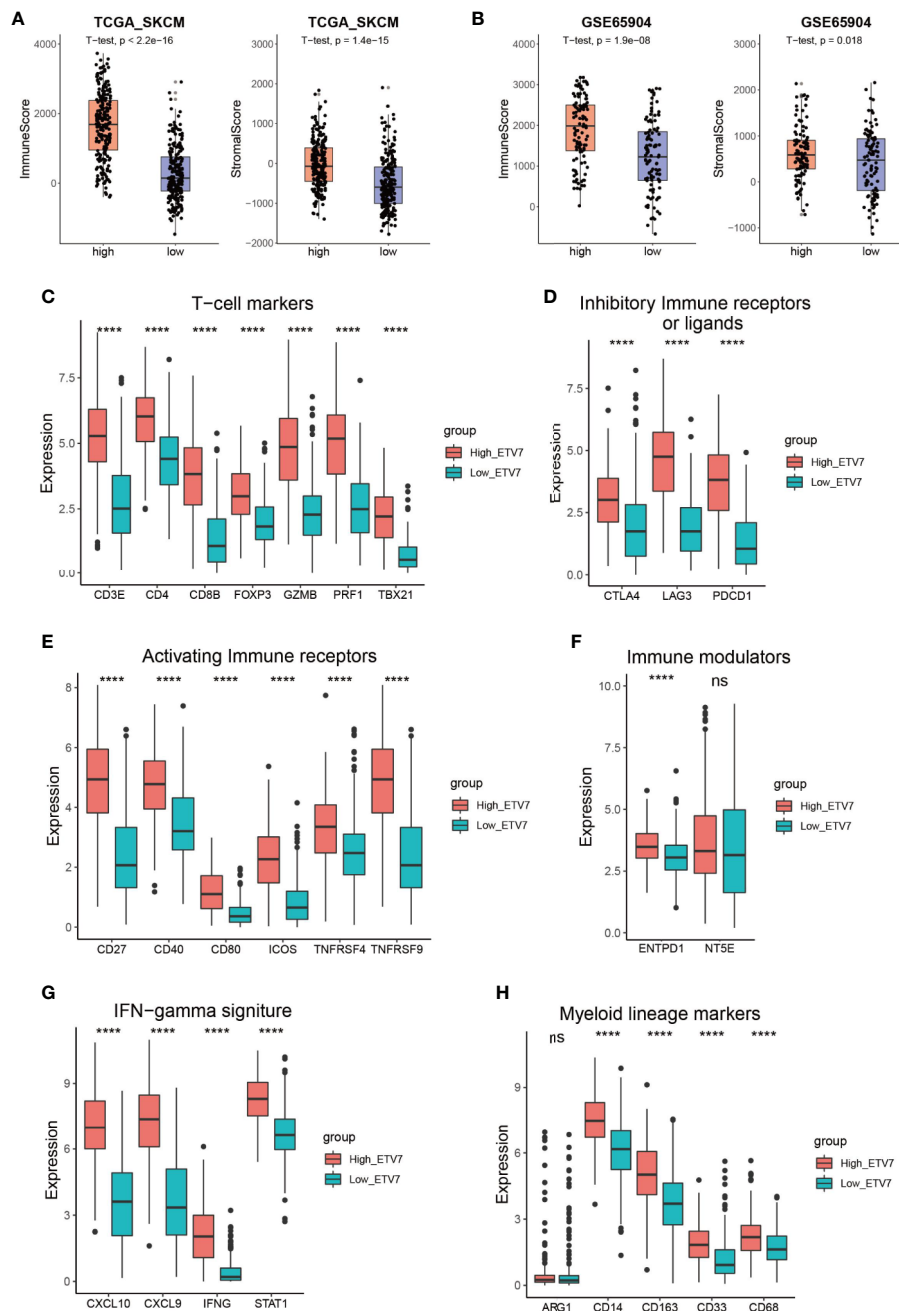


FIGURE 7 | Immune profile of melanoma patients with high and low ETV7 expression. **(A, B)** Immune and stromal scores of melanoma patients with high and low ETV7 expression in the TCGA_SKCM **(A)** and GSE65904 **(B)** cohorts. **(C–H)** Comparison of the expression of T cell markers **(C)**, inhibitory immune receptors or ligands **(D)**, activating immune receptors **(E)**, immune modulators **(F)**, IFN γ signatures **(G)**, and myeloid lineage phenotypic and functional markers **(H)** between melanoma patients with high and low ETV7 expression. ****: $p < 0.0001$. ns, no significant.

that only ETV7 had significant prognostic relevance in melanoma **(Figures 3A, J)**. Moreover, the gene could serve as an independent prognostic predictor after correcting for other confounding factors **(Table 1)**. Indeed, all patients in various subgroups of melanoma with low ETV7 expression showed a significantly shorter OS than those with high ETV7 expression **(Figure 4)**. Several studies reported that ETS1 supported cell

growth (39), prevented apoptosis (40), and facilitated the invasion of melanoma (22); however, an early study demonstrated that the gene was widely expressed in benign and malignant melanocytes, and immunohistochemical analysis indicated that its expression had no significant association with the clinical outcome (41), supporting the results of the current study. Two studies also observed that

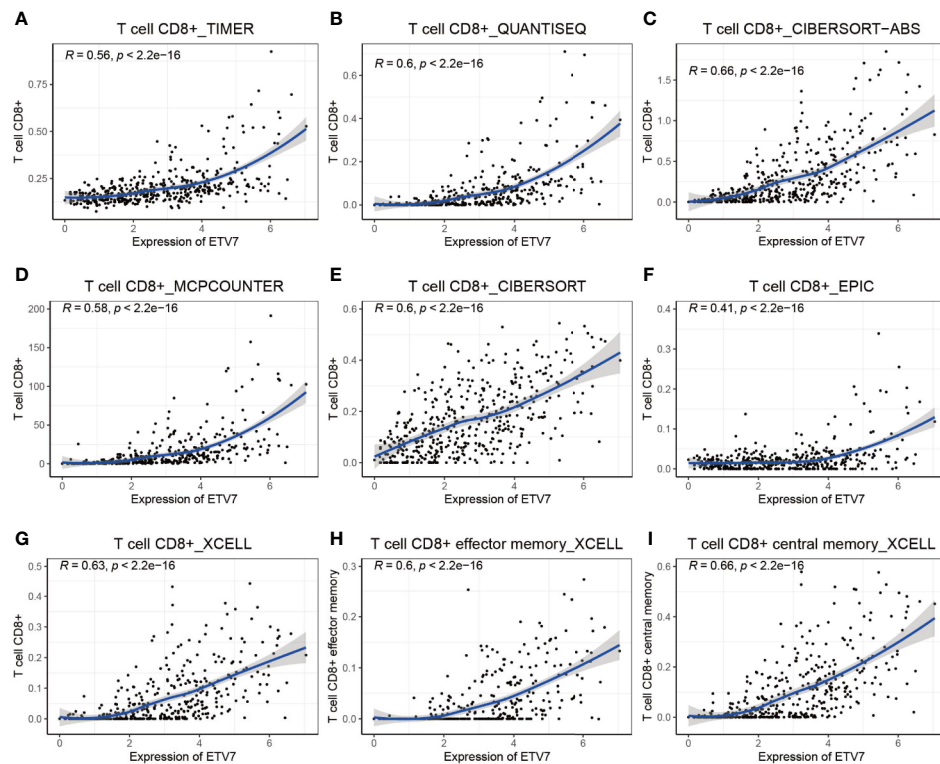


FIGURE 8 | Correlation between the expression of ETV7 and abundance of CD8+ T cells (A–I).

5.3–18% of melanoma patients exhibited an increase in ETV1 expression. Overexpression of ETV1, combined with oncogenic NRAS (G12D), can transform primary melanocytes and promote tumor formation in mice (42, 43). Although ETV1 showed no significant prognostic relevance in melanoma in the present study, its importance in a subset of melanomas with ETV1 amplification could not be underestimated and ignored. In addition, no studies have reported on the expression and function of ELK3, ETV5 ELF3, ELF5, ETS2, and SPDEF in melanoma. Although in this study, their expression was not correlated with prognosis, their involvement in the development of certain cases of melanoma could not be excluded, and future research has to be conducted.

As a member of the ETS transcription factor family, ETV7 in melanoma has not been previously investigated. Our knowledge of the gene under physiological and pathological conditions is considerably limited. Initially identified at the beginning of this century, ETV7 was found to be highly related to the oncogenic ETV6 (36). However, recent studies have found that the two genes exerted opposite biological effects, and ETV7 can inhibit the transcriptional activities of ETV6 (44, 45). ETV7 has earlier been reported to act as a hematopoietic oncoprotein; however, three recent studies found that the gene could suppress the proliferation, migration, and invasion of some solid tumors such as oral squamous cell carcinoma and nasopharyngeal carcinoma (45–49). To explore the role of ETV7 in melanoma, we analyzed seven independent melanoma-related data sets (TCGA_SKCM,

GSE65904, GSE19234, and four data sets from the cBioportal database) by conducting GSEA, GO, and KEGG analyses, which are widely used bioinformatics tools in the functional characterization of specific genes (50–53). All of these enrichment analyses suggest broad ETV7 involvement in immune-related processes and pathways, including the following: T cell activation; Th1, Th2, and Th17 cell differentiation; PD-L1 expression and PD-1 checkpoint pathway in cancer; and antigen processing and presentation (Figures 5–7). Melanoma patients with high ETV7 expression had significantly higher immune scores than those with low ETV7, suggesting higher immune cell infiltration in the tumor microenvironment. Indeed, when the infiltration of various immune cells in melanoma was estimated, ETV7 showed a strong positive correlation with the infiltration of CD8+ T cells (Figure 9). Moreover, melanoma patients with high ETV7 exhibited a significantly higher expression of various T cell markers, such as CD3E, CD4, CD8B, and TBX21 (54); this finding verified the close link between ETV7 and T cell infiltration. With the ETV7 expression in hematopoietic cells considered, the strong correlation between ETV7 and the infiltration of CD8+ T cells may be attributed to ETV7 expression in T cells rather than tumor cells. Thus, we first evaluated ETV7 expression across a set of normal human cells or tissues in the human protein atlas; the skin was found to exhibit the highest ETV7 expression. We then analyzed the public scRNA-seq data set (GSE72056) and found that most of the

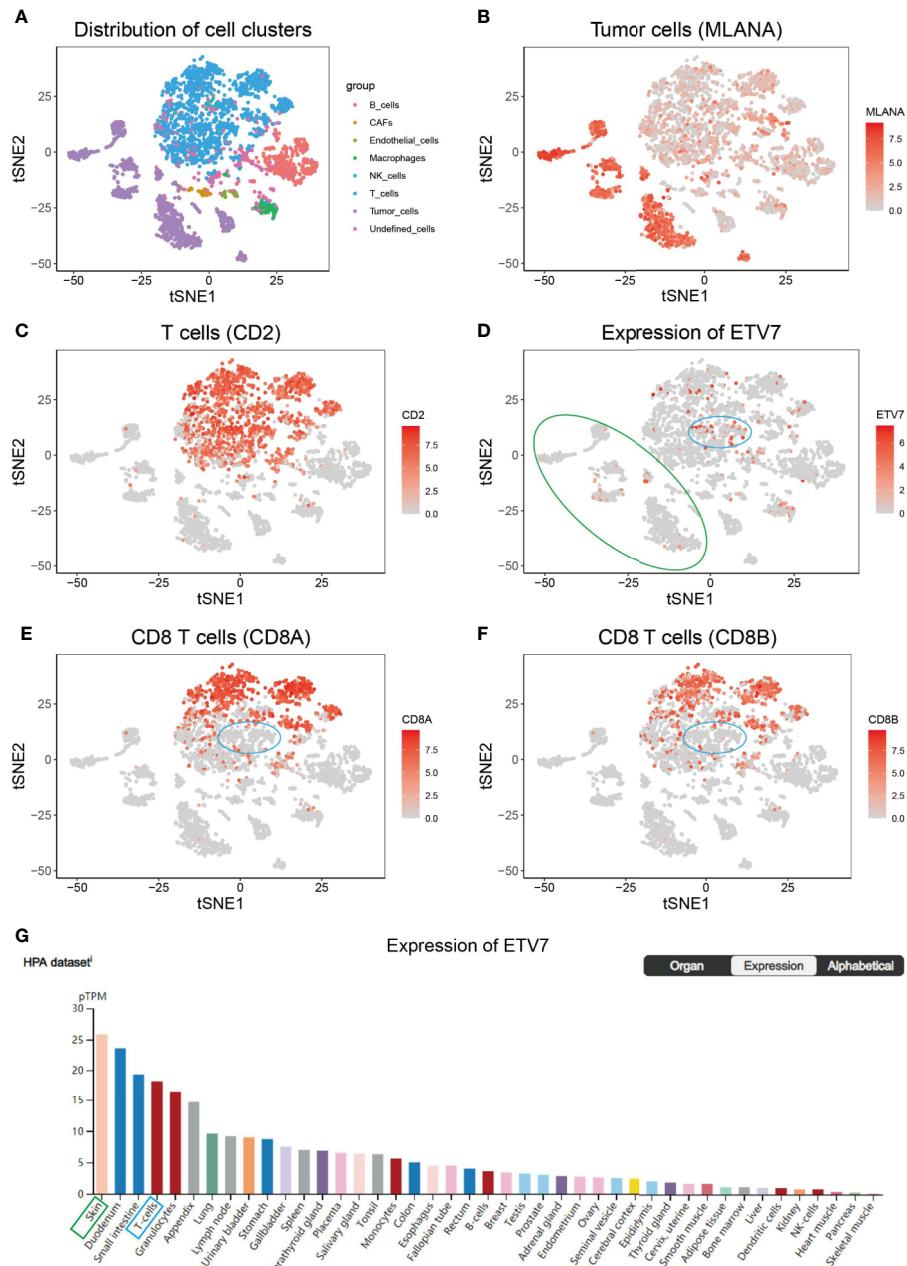


FIGURE 9 | Single-cell RNA sequencing (scRNA-seq) analysis of ETV7 in melanoma. **(A)** t-Distributed stochastic neighbor embedding (t-SNE) analysis of different clusters of cells in the GSE72056 data set. **(B)** The average expression of MLANA for tumor cells overlaid on the tSNE plot. **(C)** Average expression of CD2 for T cells overlaid on the tSNE plot. **(D)** Average expression of ETV7 for cells overlaid on the tSNE plot. **(E)** Average expression of CD8A for CD8+ T cells overlaid on the tSNE plot. **(F)** Average expression of CD8B for CD8+ T cells overlaid on the tSNE plot. **(G)** Expression of ETV7 across a set of normal human cells. (A green circle denotes cluster of tumor cells; a blue circle indicates a specific fraction of T cells).

CD8+ T cells showed no ETV7 expression, and some ETV7-positive T cells were not CD8+ T cells (**Figures 9C–F**). ETV7 could be detected in some melanoma tumor cells (**Figure 9D**). ETV7 was highly expressed in normal skin and showed markedly decreased expression in melanoma (**Figures 2L, N and 9G**); thus, not all melanoma cells might be expected to express ETV7 (**Figure 9D**).

Moreover, early studies inferred a positive regulatory role of ETV7 in T and B cells (45, 48). In the study by Cintia Carella et al., all mice that received transplants with TEL2-expressing bone marrow died from T-cell lymphoma, whereas none of the control mice developed hematopoietic malignancy with the chemical carcinogen N-ethyl-N-nitrosourea (45). Monica Cardone et al. showed that ETV7 could inhibit apoptosis and

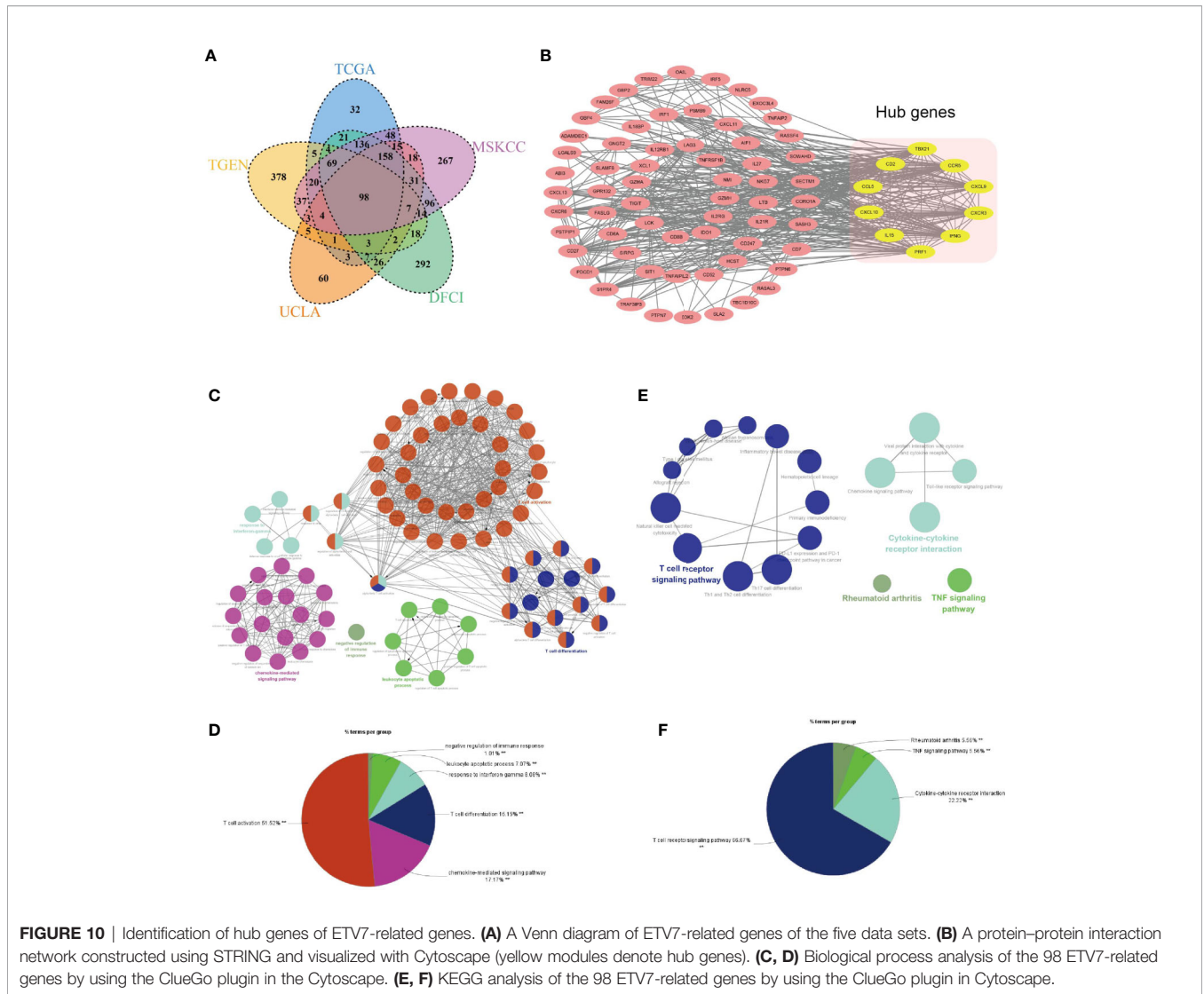


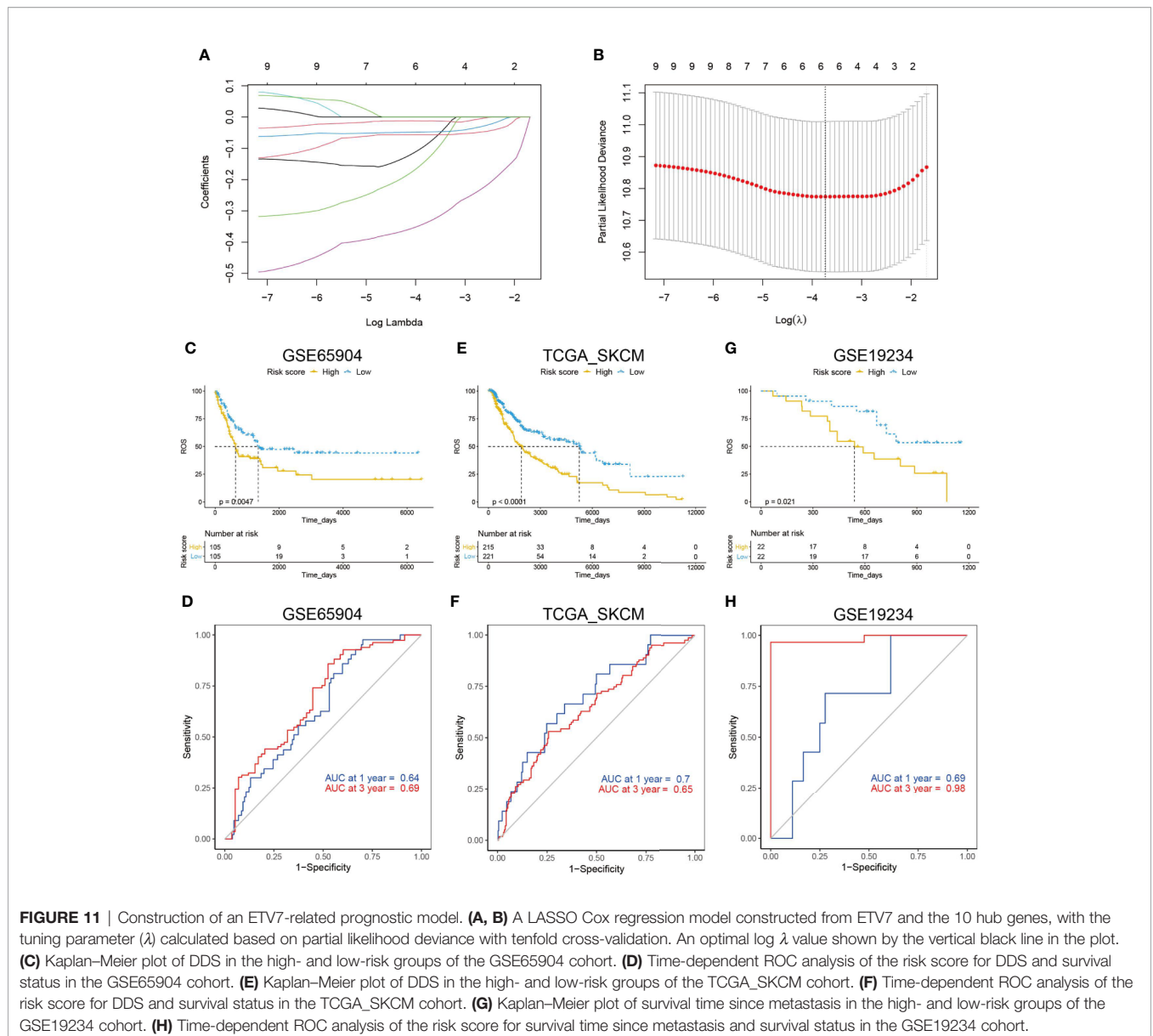
FIGURE 10 | Identification of hub genes of ETV7-related genes. **(A)** A Venn diagram of ETV7-related genes of the five data sets. **(B)** A protein–protein interaction network constructed using STRING and visualized with Cytoscape (yellow modules denote hub genes). **(C, D)** Biological process analysis of the 98 ETV7-related genes by using the ClueGo plugin in the Cytoscape. **(E, F)** KEGG analysis of the 98 ETV7-related genes by using the ClueGo plugin in Cytoscape.

promote B cell proliferation by targeting the cell cycle and apoptotic regulators (48). The results obtained from the present study, combined with other studies, highly suggest that ETV7 can have an essential role in T cell differentiation, proliferation, infiltration, and activation in melanoma.

Notably, several members of the ETS family regulate the immune system (55, 56). ETS1 regulates the differentiation of several types of immune cells, such as T helper cell subsets and cytotoxic T cells; it also directly controls the expression of cytokine and chemokine genes (57). The mechanism by which ETV7, a member of the ETS family, regulates the immune process and response in melanoma has yet to be determined. However, 10 hub genes were identified in the current study (**Figure 10B**). Among them, CD2 is a transmembrane glycoprotein typically known for its participation in the costimulatory pathway of T cell activation (58). TBX21 is essential for naive T lymphocyte development and interferon-gamma production (59). IL15 is identified as a cytokine that stimulates the proliferation of T lymphocytes (60). PRF1 encodes

the protein perforin, which is present in T and NK cells and facilitates the release of granzymes and subsequent cytolysis of target cells (61). CCR5, CXCL10, CXCR3, CXCL9, CCL5, and IFNG also participate in the migration, trafficking, or differentiation of T cells (61–65). Whether ETV7 binds the promoter of these genes and stimulates their expression remains unknown, but our analysis showed a high correlation between them and ETV7 at the transcriptional level. To clarify this concern, future studies have to be conducted.

We further constructed a prognostic model by using LASSO Cox regression, a broadly selected machine learning algorithm to minimize the risk of overfitting (66). The model had a relatively good predictive value in training and testing cohorts (**Figures 11D, F**). All six gene signatures were immune-related and regulated the proliferation, differentiation, migration, or activation of T cells (59, 60, 62, 63, 65). In addition, melanoma patients with low expression of these six gene signatures had a significantly shorter OS (**Supplementary Figure 5**). T cells, particularly CD8+ T cells, demonstrate a predominant role in



the anticancer effects of ICIs. Thus, the model can potentially help select patients who can be responsive to ICIs; however, this hypothesis should be tested by prospective analysis in multicenter cohorts.

CONCLUSIONS

A systematic analysis of the ETS family in melanoma identified an essential role of ETV7 in regulating the immune microenvironment of the disease. Further studies are recommended to explore the exact mechanism that allows ETV7 to regulate the proliferation, migration, infiltration, and activation of immune cells, particularly CD8+ T cells.

DATA AVAILABILITY STATEMENT

The original contributions presented in the study are included in the article/**Supplementary Material**. Further inquiries can be directed to the corresponding author.

AUTHOR CONTRIBUTIONS

HQ and HZ contributed equally to this work. The study was conceived and designed by ZS. Analysis of data was performed by HQ, HZ, and ZS. Bioinformatics analysis in R was conducted by ZS and XZ. Useful discussion and advice were provided by YL, FL, and LS. ZS drafted the article. All authors contributed to the article and approved the submitted version.

FUNDING

This work is supported by the New Xiangya Talent Project of the Third Xiangya Hospital of Central South University (Grant No. JY201715).

SUPPLEMENTARY MATERIAL

The Supplementary Material for this article can be found online at: <https://www.frontiersin.org/articles/10.3389/fimmu.2020.612784/full#supplementary-material>

SUPPLEMENTARY FIGURE 1 | Expression profile of the ETS family in melanoma. **(A–O)** Expression of ELF1 **(A)**, SPIC **(B)**, SPIB **(C)**, GABPA **(D)**, FLI1 **(E)**, ETV3L **(F)**, ETV3 **(G)**, ETV2 **(H)**, FEV **(I)**, ETV6 **(J)**, ERF **(K)**, ELK4 **(L)**, ELK1 **(M)**, ELF4 **(N)**, and ELF2 **(O)** in melanoma and corresponding normal tissues, based on the GEPIA2 database. **(P–S)**. Data from the OncoPrint database show that EHF

(P), SPI1 **(Q)**, ETV4 **(R)**, and ERG **(S)** are not differentially expressed between tumor and normal tissues across three cohorts.

SUPPLEMENTARY FIGURE 2 | Prognostic analysis of the differentially expressed genes of the ETS family in melanoma. **(A–H)** Kaplan–Meier plot of overall survival in melanoma patients in the GSE65904 cohort with high and low expression of ELF3 **(A)**, SPDEF **(B)**, ETV5 **(C)**, ETV1 **(D)**, ETS2 **(E)**, ETS1 **(F)**, ELK3 **(G)**, or ELF5 **(H)**.

SUPPLEMENTARY FIGURE 3 | GO enrichment analysis of ETV7-related genes in the TCGA_SKCM **(A)**, MSKCC NEJM **(B)**, DFCI Science **(C)**, UCLA Cell **(D)**, TGEN Genome Res **(E)**, and GSE19234 **(F)** data sets.

SUPPLEMENTARY FIGURE 4 | Single-cell RNA sequencing (scRNA-seq) analysis in melanoma. **(A)** Average expression of CD163 for macrophages overlaid on the tSNE plot. **(B)** Average expression of CD19 for B cells overlaid on the tSNE plot. **(C)** Expression of ETV7 across a set of normal human tissues.

SUPPLEMENTARY FIGURE 5 | Prognostic analysis of ETV7-related hub genes in melanoma. **(A–J)** Kaplan–Meier plot of overall survival of melanoma patients in the TCGA_SKCM cohort with high and low expression of CCL5 **(A)**, TBX21 **(B)**, PRR1 **(C)**, IL15 **(D)**, IFNG **(E)**, CXCR3 **(F)**, CXCL10 **(G)**, CXCL9 **(H)**, CD2 **(I)**, or CCR5 **(J)**.

REFERENCES

- Schadendorf D, Hauschild A. Melanoma in 2013: Melanoma—the run of success continues. *Nat Rev Clin Oncol* (2014) 11(2):75–6. doi: 10.1038/nrclinonc.2013.246
- Siegel RL, Miller KD, Jemal A. Cancer statistics, 2019. *CA: A Cancer J Clin* (2019) 69(1):7–34. doi: 10.3322/caac.21551
- Furie M, Ito T, Wada N, Wada M, Kadono T, Uchi H. Melanoma and Immune Checkpoint Inhibitors. *Curr Oncol Rep* (2018) 20(3):29. doi: 10.1007/s11912-018-0676-z
- Syn NL, Teng MWL, Mok TSK, Soo RA. De-novo and acquired resistance to immune checkpoint targeting. *Lancet Oncol* (2017) 18(12):e731–41. doi: 10.1016/S1470-2045(17)30607-1
- Gide TN, Wilmott JS, Scolyer RA, Long GV. Primary and Acquired Resistance to Immune Checkpoint Inhibitors in Metastatic Melanoma. *Clin Cancer Res* (2018) 24(6):1260–70. doi: 10.1158/1078-0432.CCR-17-2267
- Diaz-Martinez M, Benito-Jardon L, Alonso L, Koetz-Ploch L, Hernando E, Teixeira J. miR-204-5p and miR-211-5p Contribute to BRAF Inhibitor Resistance in Melanoma. *Cancer Res* (2018) 78(4):1017–30. doi: 10.1158/0008-5472.CAN-17-1318
- Hugo W, Shi H, Sun L, Piva M, Song C, Kong X, et al. Non-genomic and Immune Evolution of Melanoma Acquiring MAPKi Resistance. *Cell* (2015) 162(6):1271–85. doi: 10.1016/j.cell.2015.07.061
- Shi H, Moriceau G, Kong X, Lee MK, Lee H, Koya RC, et al. Melanoma whole-exome sequencing identifies (V600E)B-RAF amplification-mediated acquired B-RAF inhibitor resistance. *Nat Commun* (2012) 3:724. doi: 10.1038/ncomms1727
- Wang B, Krall EB, Aguirre AJ, Kim M, Widlund HR, Doshi MB, et al. ATXN1L, CIC, and ETS Transcription Factors Modulate Sensitivity to MAPK Pathway Inhibition. *Cell Rep* (2017) 18(6):1543–57. doi: 10.1016/j.celrep.2017.01.031
- Echevarria-Vargas IM, Reyes-Urbe PI, Guterres AN, Yin X, Kossenkov AV, Liu Q, et al. Co-targeting BET and MEK as salvage therapy for MAPK and checkpoint inhibitor-resistant melanoma. *EMBO Mol Med* (2018) 10(5):e8446. doi: 10.15252/emmm.201708446
- Johannessen CM, Johnson LA, Piccioni F, Townes A, Frederick DT, Donahue MK, et al. A melanocyte lineage program confers resistance to MAP kinase pathway inhibition. *Nature* (2013) 504(7478):138–42. doi: 10.1038/nature12688
- Taylor JM, Dupont-Versteegden EE, Davies JD, Hassell JA, Houle JD, Gurley CM, et al. A role for the ETS domain transcription factor PEA3 in myogenic differentiation. *Mol Cell Biol* (1997) 17(9):5550–8. doi: 10.1128/MCB.17.9.5550
- Samakovlis C, Hacohen N, Manning G, Sutherland DC, Guillemin K, Krasnow MA. Development of the Drosophila tracheal system occurs by a series of morphologically distinct but genetically coupled branching events. *Development* (1996) 122(5):1395–407. doi: 10.1002/(SICI)1097-0320(19960501)24:1<93::AID-CYTO11>3.0.CO;2-Q
- Treisman R. Ternary complex factors: growth factor regulated transcriptional activators. *Curr Opin Genet Dev* (1994) 4(1):96–101. doi: 10.1016/0959-437X(94)90097-3
- Selvaraj N, Kedage V, Hollenhorst PC. Comparison of MAPK specificity across the ETS transcription factor family identifies a high-affinity ERK interaction required for ERG function in prostate cells. *Cell Communication Signaling* (2015) 13(1):12. doi: 10.1186/s12964-015-0089-7
- Charlot C, Dubois-Pot H, Serchov T, Tourrette Y, Wasylyk B. A review of post-translational modifications and subcellular localization of Ets transcription factors: possible connection with cancer and involvement in the hypoxic response. *Methods Mol Biol* (2010) 647:3–30. doi: 10.1007/978-1-60761-738-9_1
- Luk IY, Reehorst CM, Mariadason JM. ELF3, ELF5, EHF and SPDEF Transcription Factors in Tissue Homeostasis and Cancer. *Molecules* (2018) 23(9):2191. doi: 10.3390/molecules23092191
- Hsing M, Wang Y, Rennie PS, Cox ME, Cherkasov A. ETS transcription factors as emerging drug targets in cancer. *Med Res Rev* (2020) 40(1):413–30. doi: 10.1002/med.21575
- Pop MS, Stransky N, Garvie CW, Theurillat JP, Hartman EC, Lewis TA, et al. A small molecule that binds and inhibits the ETV1 transcription factor oncoprotein. *Mol Cancer Ther* (2014) 13(6):1492–502. doi: 10.1158/1535-7163.MCT-13-0689
- Butler MS, Roshan-Moniri M, Hsing M, Lau D, Kim A, Yen P, et al. Discovery and characterization of small molecules targeting the DNA-binding ETS domain of ERG in prostate cancer. *Oncotarget* (2017) 8(26):42438–54. doi: 10.18632/oncotarget.17124
- Potu H, Peterson LF, Kandarpa M, Pal A, Sun H, Durham A, et al. Usp9x regulates Ets-1 ubiquitination and stability to control NRAS expression and tumorigenicity in melanoma. *Nat Commun* (2017) 8:14449. doi: 10.1038/ncomms14449
- Rothhammer T, Hahne JC, Florin A, Poser I, Soncin F, Wernert N, et al. The Ets-1 transcription factor is involved in the development and invasion of malignant melanoma. *Cell Mol Life Sci* (2004) 61(1):118–28. doi: 10.1007/s00018-003-3337-8
- Baltrunaite K, Craig MP, Palencia Desai S, Chaturvedi P, Pandey RN, Hegde RS, et al. ETS transcription factors ETV2 and Fli1b are required for tumor angiogenesis. *Angiogenesis* (2017) 20(3):307–23. doi: 10.1007/s10456-017-9539-8
- Liu M, Gao W, van Velkinburgh JC, Wu Y, Ni B, Tian Y. Role of Ets Proteins in Development, Differentiation, and Function of T-Cell Subsets. *Med Res Rev* (2016) 36(2):193–220. doi: 10.1002/med.21361
- Cao Q, Yang S, Lv Q, Liu Y, Li L, Wu X, et al. Five ETS family members, ELF-1, ETV-4, ETV-3L, ETS-1, and ETS-2 upregulate human leukocyte-associated immunoglobulin-like receptor-1 gene basic promoter activity. *Aging (Albany NY)* (2018) 10(6):1390–401. doi: 10.18632/aging.101475
- Wang H, Jain S, Li P, Lin JX, Oh J, Qi C, et al. Transcription factors IRF8 and PU.1 are required for follicular B cell development and BCL6-driven germinal center responses. *Proc Natl Acad Sci USA* (2019) 116(19):9511–20. doi: 10.1073/pnas.1901258116
- Verbrugge A, Rijkers ES, de Ruiter T, Meyaard L. Leukocyte-associated Ig-like receptor-1 has SH2 domain-containing phosphatase-independent function and recruits C-terminal Src kinase. *Eur J Immunol* (2006) 36(1):190–8. doi: 10.1002/eji.200535226

28. Yamada T, Park CS, Mamonkin M, Lacorazza HD. Transcription factor ELF4 controls the proliferation and homing of CD8+ T cells via the Kruppel-like factors KLF4 and KLF2. *Nat Immunol* (2009) 10(6):618–26. doi: 10.1038/ni.1730
29. Zhang J, Zhang X, Li J, Song Z. Systematic analysis of the ABC transporter family in hepatocellular carcinoma reveals the importance of ABCB6 in regulating ferroptosis. *Life Sci* (2020) 257:118131. doi: 10.1016/j.lfs.2020.118131
30. Tirosh I, Izar B, Prakadan SM, Wadsworth MH 2nd, Treacy D, Trombetta JJ. Dissecting the multicellular ecosystem of metastatic melanoma by single-cell RNA-seq. *Science* (2016) 352(6282):189–96. doi: 10.1126/science.aad0501
31. Yoshihara K, Shahmoradgoli M, Martinez E, Vegesna R, Kim H, Torres-Garcia W, et al. Inferring tumour purity and stromal and immune cell admixture from expression data. *Nat Commun* (2013) 4:2612. doi: 10.1038/ncomms3612
32. Li T, Fan J, Wang B, Traugh N, Chen Q, Liu JS, et al. TIMER: A Web Server for Comprehensive Analysis of Tumor-Infiltrating Immune Cells. *Cancer Res* (2017) 77(21):e108–10. doi: 10.1158/0008-5472.CAN-17-0307
33. Tang Z, Kang B, Li C, Chen T, Zhang Z. GEPIA2: an enhanced web server for large-scale expression profiling and interactive analysis. *Nucleic Acids Res* (2019) 47(W1):W556–60. doi: 10.1093/nar/gkz430
34. Sturm G, Finotello F, Petitprez F, Zhang JD, Baumbach J, Fridman WH, et al. Comprehensive evaluation of transcriptome-based cell-type quantification methods for immuno-oncology. *Bioinformatics* (2019) 35(14):i436–45. doi: 10.1093/bioinformatics/btz363
35. Li B, Severson E, Pignon JC, Zhao H, Li T, Novak J, et al. Comprehensive analyses of tumor immunity: implications for cancer immunotherapy. *Genome Biol* (2016) 17(1):174. doi: 10.1186/s13059-016-1028-7
36. Potter MD, Buijs A, Kreider B, van Rompaey L, Grosveld GC. Identification and characterization of a new human ETS-family transcription factor, TEL2, that is expressed in hematopoietic tissues and can associate with TEL1/ETV6. *Blood* (2000) 95(11):3341–8. doi: 10.1182/blood.V95.11.3341.011k44_3341_3348
37. Numata M, Klein Geltink RI, Grosveld GC. Establishment of a transgenic mouse to model ETV7 expressing human tumors. *Transgenic Res* (2019) 28(1):115–28. doi: 10.1007/s11248-018-0104-z
38. Bindea G, Mlecnik B, Hackl H, Charoentong P, Tosolini M, Kirilovsky A, et al. ClueGO: a Cytoscape plug-in to decipher functionally grouped gene ontology and pathway annotation networks. *Bioinformatics* (2009) 25(8):1091–3. doi: 10.1093/bioinformatics/btp101
39. Kubic JD, Little EC, Lui JW, Iizuka T, Lang D. PAX3 and ETS1 synergistically activate MET expression in melanoma cells. *Oncogene* (2015) 34(38):4964–74. doi: 10.1038/ncr.2014.420
40. Dong L, Jiang CC, Thorne RF, Croft A, Yang F, Liu H, et al. Ets-1 mediates upregulation of Mcl-1 downstream of XBP-1 in human melanoma cells upon ER stress. *Oncogene* (2011) 30(34):3716–26. doi: 10.1038/ncr.2011.87
41. Torlakovic EE, Bilalovic N, Nesland JM, Torlakovic G, Florenes VA. Ets-1 transcription factor is widely expressed in benign and malignant melanocytes and its expression has no significant association with prognosis. *Mod Pathol* (2004) 17(11):1400–6. doi: 10.1038/modpathol.3800206
42. Jane-Valbuena J, Widlund HR, Perner S, Johnson LA, Dibner AC, Lin WM, et al. An oncogenic role for ETV1 in melanoma. *Cancer Res* (2010) 70(5):2075–84. doi: 10.1158/0008-5472.CAN-09-3092
43. Mehra R, Dhanasekaran SM, Palanisamy N, Vats P, Cao X, Kim JH, et al. Comprehensive Analysis of ETS Family Members in Melanoma by Fluorescence In Situ Hybridization Reveals Recurrent ETV1 Amplification. *Transl Oncol* (2013) 6(4):405–12. doi: 10.1593/tlo.13340
44. Vivekanand P, Rebay I. The SAM domain of human TEL2 can abrogate transcriptional output from TEL1 (ETV-6) and ETS1/ETS2. *PLoS One* (2012) 7(5):e37151. doi: 10.1371/journal.pone.0037151
45. Carella C, Potter M, Bonten J, Rehng JE, Neale G, Grosveld GC. The ETS factor TEL2 is a hematopoietic oncoprotein. *Blood* (2006) 107(3):1124–32. doi: 10.1182/blood-2005-03-1196
46. Salameti V, Bhosale PG, Ames-Draycott A, Sipilä K, Watt FM. NOTCH1 signaling in oral squamous cell carcinoma via a TEL2/SERPINE1 axis. *Oncotarget* (2019) 10(63):6791–804. doi: 10.18632/oncotarget.27306
47. Sang Y, Cheng C, Zeng YX, Kang T. Snail promotes metastasis of nasopharyngeal carcinoma partly by down-regulating TEL2. *Cancer Commun (Lond)* (2018) 38(1):58. doi: 10.1186/s40880-018-0328-6
48. Cardone M, Kandilci A, Carella C, Nilsson JA, Brennan JA, Sirma S, et al. The novel ETS factor TEL2 cooperates with Myc in B lymphomagenesis. *Mol Cell Biol* (2005) 25(6):2395–405. doi: 10.1128/MCB.25.6.2395-2405.2005
49. Sang Y, Chen MY, Luo D, Zhang RH, Wang L, Li M, et al. TEL2 suppresses metastasis by down-regulating SERPINE1 in nasopharyngeal carcinoma. *Oncotarget* (2015) 6(30):29240–53. doi: 10.18632/oncotarget.5074
50. Mootha VK, Lindgren CM, Eriksson KF, Subramanian A, Sihag S, Lehar J, et al. PGC-1 α -responsive genes involved in oxidative phosphorylation are coordinately downregulated in human diabetes. *Nat Genet* (2003) 34(3):267–73. doi: 10.1038/ng1180
51. Subramanian A, Tamayo P, Mootha VK, Mukherjee S, Ebert BL, Gillette MA, et al. Gene set enrichment analysis: a knowledge-based approach for interpreting genome-wide expression profiles. *Proc Natl Acad Sci USA* (2005) 102(43):15545–50. doi: 10.1073/pnas.0506580102
52. The Gene Ontology, C. Expansion of the Gene Ontology knowledgebase and resources. *Nucleic Acids Res* (2017) 45(D1):D331–8. doi: 10.1093/nar/gkw1108
53. Kanehisa M, Sato Y, Kawashima M, Furumichi M, Tanabe M. KEGG as a reference resource for gene and protein annotation. *Nucleic Acids Res* (2016) 44(D1):D457–62. doi: 10.1093/nar/gkv1070
54. Zheng S, Zou Y, Liang JY, Xiao W, Yang A, Meng T, et al. Identification and validation of a combined hypoxia and immune index for triple-negative breast cancer. *Mol Oncol* (2020) 14(11):2814–33. doi: 10.1002/1878-0261.12747
55. Gallant S, Gilkeson G. ETS transcription factors and regulation of immunity. *Arch Immunol Ther Exp (Warsz)* (2006) 54(3):149–63. doi: 10.1007/s00005-006-0017-z
56. Suico MA, Shuto T, Kai H. Roles and regulations of the ETS transcription factor ELF4/MEF. *J Mol Cell Biol* (2017) 9(3):168–77. doi: 10.1093/jmcb/mjw051
57. Russell L, Garrett-Sinha LA. Transcription factor Ets-1 in cytokine and chemokine gene regulation. *Cytokine* (2010) 51(3):217–26. doi: 10.1016/j.cyto.2010.03.006
58. Binder C, Cvetkovski F, Sellberg F, Berg S, Paternina Visbal H, Sachs DH, et al. CD2 Immunobiology. *Front Immunol* (2020) 11:1090. doi: 10.3389/fimmu.2020.01090
59. Sharma N, Jaiswal I, Mandal RK, Phadke SR, Awasthi S. Genetic variation of TBX21 gene increases risk of asthma and its severity in Indian children. *J Hum Genet* (2014) 59(8):437–43. doi: 10.1038/jhg.2014.52
60. Grabstein KH, Eisenman J, Shanebeck K, Rauch C, Srinivasan S, Fung V, et al. Cloning of a T cell growth factor that interacts with the beta chain of the interleukin-2 receptor. *Science* (1994) 264(5161):965–8. doi: 10.1126/science.8178155
61. Wang T, Sun G, Wang Y, Li S, Zhao X, Zhang C, et al. The immunoregulatory effects of CD8 T-cell-derived perforin on diet-induced nonalcoholic steatohepatitis. *FASEB J* (2019) 33(7):8490–503. doi: 10.1096/fj.201802534RR
62. Li R, Zhang N, Tian M, Ran Z, Zhu M, Zhu H, et al. Temporary CXCR3 and CCR5 antagonism following vaccination enhances memory CD8 T cell immune responses. *Mol Med* (2016) 22:497–507. doi: 10.2119/molmed.2015.00218
63. House IG, Savas P, Lai J, Chen AXY, Oliver AJ, Teo ZL, et al. Macrophage-Derived CXCL9 and CXCL10 Are Required for Antitumor Immune Responses Following Immune Checkpoint Blockade. *Clin Cancer Res* (2020) 26(2):487–504. doi: 10.1158/1078-0432.CCR-19-1868
64. Huffman AP, Lin JH, Kim SI, Byrne KT, Vonderheide RH. CCL5 mediates CD40-driven CD4+ T cell tumor infiltration and immunity. *JCI Insight* (2020) 5(10):e137263. doi: 10.1172/jci.insight.137263
65. Krummel MF, Mahale JN, Uhl LFK, Hardison EA, Mujal AM, Mazet JM, et al. Paracrine costimulation of IFN- γ signaling by integrins modulates CD8 T cell differentiation. *Proc Natl Acad Sci USA* (2018) 115(45):11585–90. doi: 10.1073/pnas.1804556115
66. Gui J, Li H. Penalized Cox regression analysis in the high-dimensional and low-sample size settings, with applications to microarray gene expression data. *Bioinformatics* (2005) 21(13):3001–8. doi: 10.1093/bioinformatics/bti422

Conflict of Interest: The authors declare that the research was conducted in the absence of any commercial or financial relationships that could be construed as a potential conflict of interest.

Copyright © 2020 Qu, Zhao, Zhang, Liu, Li, Sun and Song. This is an open-access article distributed under the terms of the Creative Commons Attribution License (CC BY). The use, distribution or reproduction in other forums is permitted, provided the original author(s) and the copyright owner(s) are credited and that the original publication in this journal is cited, in accordance with accepted academic practice. No use, distribution or reproduction is permitted which does not comply with these terms.